# SYSTEMATIC STUDY TO REDUCE THE EFFECTS OF CRACKS IN MULTILAYER INSULATION PART 2: EXPERIMENTAL RESULTS<sup>a</sup>

#### O.S. Shu\*, R.W. Fast and H.L. Hart

Fermi National Accelerator Laboratory, Batavia, IL 60510, USA \* Cryogenic Laboratory, Zhejiang University, Hangzhou, People's Republic of China

Received 77 November 1986

A series of cracks with different widths and shapes was cut in a multilayer insulation (MLI) blanket. The measured data shows that the incremental heat load per unit slot area has a maximum of  $\approx 135 \, \mathrm{Wm}^{-2}$ . The heat load increment is essentially independent of the preparation of the cold surface under the crack, i.e. its emissivity, if the slot width is sufficiently small. The temperature distribution and the equivalent thermal conductivity near the cracks are quite different from that in a system without cracks. The dependence of the heat load and temperature distribution on the vacuum pressure was also observed. A systematic study of a crack-covering 'patch' method to reduce the heat load to a 77 K surface through cracks in a MLI blanket was conducted. The following patch materials were used to determine the optimum distribution of the patches in a 30 layer blanket:  $300 \, \text{Å}^b$  single aluminized crinkled Mylar (NRC-2) and  $1000 \, \text{Å}$  double aluminized flat Mylar. The experimental results indicated that the use of a patch every few layers is almost as effective as using a patch every layer. Placing the patches in the upper half of the blanket is much better than in the lower half and can reduce the heat load essentially to that without cracks. Putting the same number of patches on top of a crack is much less effective. The data suggest that  $1000 \, \text{Å}$  material is preferable for patches. All of the experimental results are generally in agreement with the enhanced black cavity model.

Keywords: multilayer insulation; heat transfer; thermal conductivity

A theoretical model, the so-called enhanced black cavity model developed in Part 1 of the paper<sup>1</sup>, has explained the unexpectedly large heat flux due to cracks in a multilayer insulation (MLI) blanket. The model can be of assistance when seeking methods to reduce this often significant effect. In the Superconducting Super Collider  $(SSC)^{2.3}$  for example, there will be 8400 superconducting dipole magnets, having a total surface area of  $2.3 \times 10^6$  m<sup>2</sup>, to which MLI will be applied with inevitable gaps, overlaps and penetrations. In large cryogenic devices<sup>4,6</sup> there are almost always some assembly joints, e.g. gaps between prewrapped MLI blankets. All of these cracks are potential sources of high heat load. We have experimentally studied the effects of cracks on the thermal performance of a MLI insulation and methods to reduce the heat load from cracks. The main goals of our investigation were:

- 1 to study the effect of cracks on the heat flux with different crack dimensions, as a function of vacuum pressure. For this study we defined a slot to be a rectangular crack, a slit to be a one-dimensional slot and a square hole to be a slot with approximately equal dimensions;
- 2 to study different crack-covering patches to find the patch material and distribution which, in a 30 layer MLI blanket, will most reduce the heat load due to cracks, as a function of vacuum pressure; and
- 3 to measure the temperature distribution in MLI blankets with cracks and to calculate the equivalent thermal conductivity in the region of cracks to understand more completely the mechanism of heat transfer in such cases.

We realize that there are many different combinations of crack dimensions, patch material and distribution which could have been tested. Several typical ones were chosen for our study, but the experimental results are of general applicability. Finally, it should be noted that we have idealized the situation by maintaining a certain distance between the MLI blanket and the warm wall in our experimental apparatus. We have taken into account the associated view factor<sup>1,7</sup>.

<sup>&</sup>lt;sup>a</sup> Work sponsored by Universities Research Associations under contract with the US Department of Energy

<sup>&</sup>lt;sup>b</sup> Å=0.1nm

#### **EXPERIMENTAL ARRANGEMENT**

#### Experimental apparatus

The experimental apparatus will be discussed only brierfly, here, since it was described in detail in a previous paper<sup>8</sup>. The black painted<sup>c</sup> inner copper plate, with an area of 2.26 m<sup>2</sup>, was refrigerated to 77 K by a thermosiphon tube connected to the liquid nitrogen supply and boil-off vessel. Individual aluminized Mylar multilayers were vertically hung on the inner plate. The temperature of the outer (warm) box was automatically maintained at 277 K.

The insulating vacuum was read by a cold cathode gauge mounted directly on the warm box inside the vacuum space. The vacuum level and residual gas species in the vacuum space can be controlled<sup>9</sup> to simulate a leak in a liquid nitrogen shielded cryogenic device. The accuracy of the wet test meter used for the nitrogen gas boil-off is  $\pm 0.2\%$ . The temperatures at different points in the superinsulation blanket and of the fin, guard vessel and guard shield were also measured and recorded during the tests.

# Cutting of cracks in the MLI blanket

Cracks of various widths and lengths were cut in the MLI blanket. An adjustable frame of Micarta bars was used to cut accurately sized cracks in the fluffy MLI blanket. The gap between the bars was exactly the width desired. The bars were clamped to the test fin at each end taking special care not to damage the MLI on the back side; they must be held firmly while cutting, so that the layers of insulation will not be pulled and torn instead of cut by the blade. A curved scalpel blade cut the MLI very well. A  $254 \times 254$ mm² Mylar sheet was inserted between the first layer and cold fin to provide a good cutting surface and to protect the surface of the fin. The size and area of the cracks were measured with an optical transit. The location of the slots in the superinsulation blanket is shown in Figure 1. There were 14 slots in two columns on the front side. i.e. opposite the thermosiphon tube, and 14 slits (a slot of zero width) on the back or tube side. The slits, cut to speed pump-down, had the same length as the slots and were symetrically located. The same method was used to cut square holes with the same area as the 4 mm slots. Figure 2 shows the slots and the square holes.

It is well-known that the thermal performance of a superinsulation blanket is quite sensitive to the wrapping technique, specifically the wrapping tension<sup>10-12</sup>, which may not be reproducible. To avoid this source of error one 30 layer MLI blanket was used for the seven runs to determine the effect of slot width on thermal performance, by starting with the narrowest slot and progressively enlarging it. Another blanket was used for the runs associated with heal load reduction methods and a third to study square holes.

## Installation of patches

The use of aluminized Mylar patches to cover cracks in a 30 layer blanket and reduce the heat load was investigated. The variables were the total number of patches and the distribution of patches within the MLI blanket. Two materials were used for the patches:  $6.4 \mu m$  crinkled single aluminized Mylar (SAMC) with 300 Å aluminizing, and  $6.4 \mu m$  flat double aluminized Mylar with 500 Å aluminizing on each side (DAM).

The patches were centred over the slots and square holes with a 10 mm overlap and secured with tape. The installation of patches within the MLI blanket must be done very carefully to achieve consistent results. For example, one should avoid getting fingerprints on the patches. The original structure of the MLI blanket should be disturbed as little as possible while installing patches. A vacuum patch-holder was made specially for this purpose.

<sup>&</sup>lt;sup>c</sup> Black-Out' high-speed opaquing solution, from Hampton Products Corporation, Fairchild, New Jersey, USA

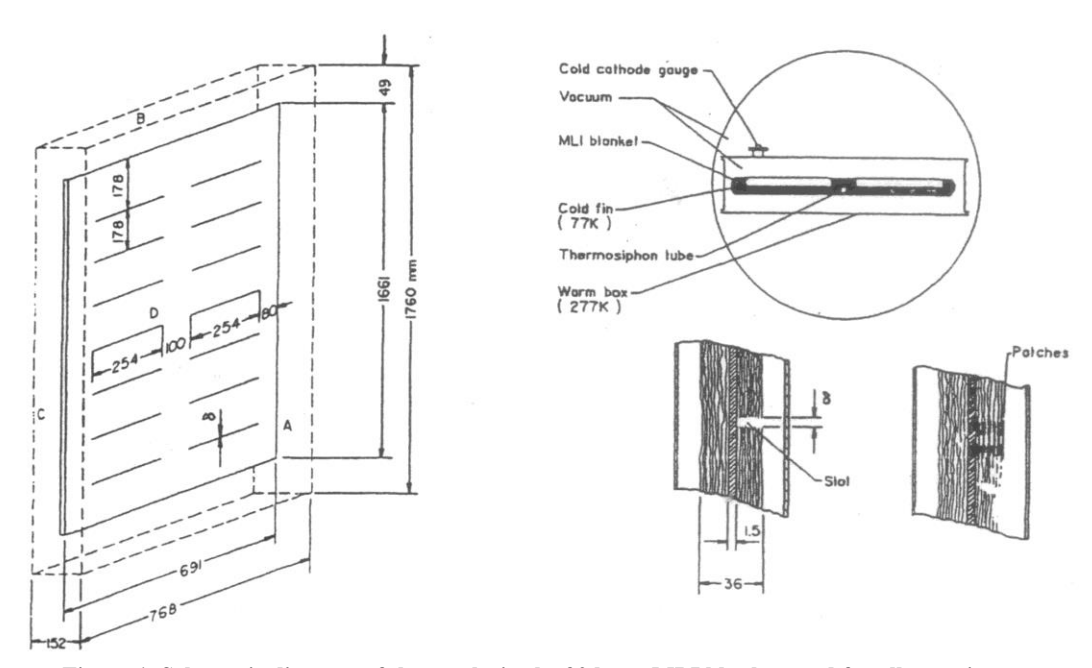
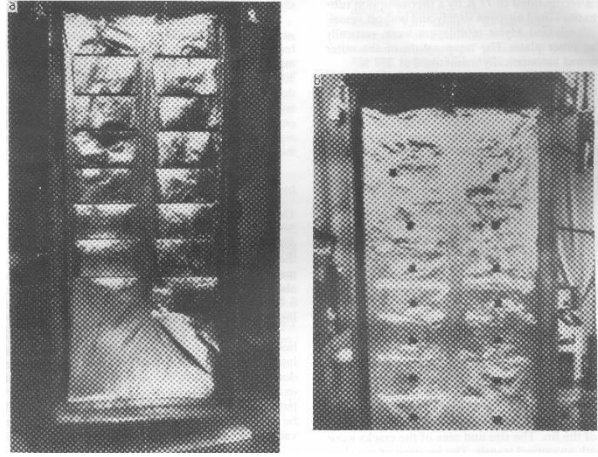


Figure 1 Schematic diagram of the cracks in the 30 layer MLI blanket used for all experiments



Fiure 2 Photograph of test apparatus showing:(a) slots and (b) square holes cut in the MLI blanket

# Temperature measurements in the MLI blanket

Since the temperature distribution helps one to understand the heat transfer mechanism in a MLI blanket, the temperature at different positions was measured with thermocouples of 0.12 mm copper and 0.12 mm constantan. The thermocouples were placed symmetrically on both sides of the inner plate. They were mounted with aluminium tape to layers 5,15,25 and 30 of all test blankets. The junction was 3 mm from the edge of slot and almost in the longitudinal centre, as shown in Figure 3. For the outermost layer (the thirtieth in Figure 3) the junction was taped at the centre of the patch.

All of the thermocouples wires were led out of the cryostat to a scanner without joints or splices to avoid the errors due to thermovoltages. The wires from the themocouples inside the MLI blanket come out of a small cut in the blanket near the top of the fin and were attached to the layer there as a heat sink.

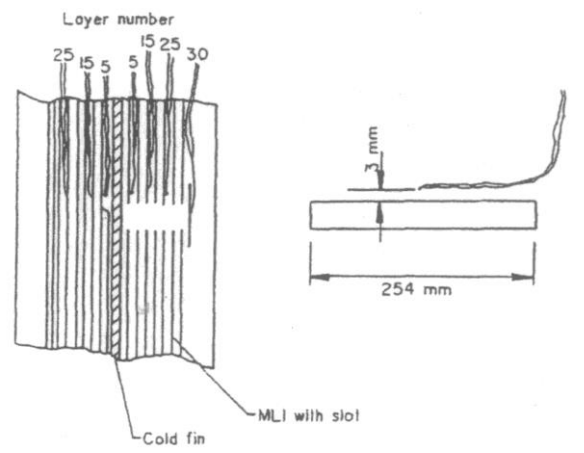


Figure 3 Schematic diagram of the thermocouples installed in MLI blanket

#### EXPERIMENTAL RESULTS: (1) EFFECTS OF SLOTS AND HOLES

## Dependence on properties of cold surface

Two tests were conducted to experimentally verify the enhanced black cavity model. If the theoretical model is of universal applicability, the unexpected, large heat load through the slots in a MLI blanket will be independent within a factor of two of the heat absorbing properties of the cold surface. Both tests had fourteen  $4 \times 254 \text{ mm}^2$  slots of the same geometry in a 30 layer MLI blanket. In one case the cold copper surface was painted black; in the other it was covered with 3M no. 425 aluminium tape.

Relevant data reported earlier<sup>7</sup> are: 1, the heat flux,  $Q_0$ , from a 277 K copper box to a black painted fin through 30 layers of MLI without cracks is 1.4 W; 2, the heat flux,  $Q_b$ , from the same box to the same black fin without MLI is 61.3 W; and 3, the heat flux,  $Q_a$ , from the same box to an aluminium taped fin without MLI is 10.9 W. The surface area, A, of the fin is 2.26 m² and the total area of slots,  $\Delta A$ , (using the optically measured widths) is 0.0114 m². The experimental results are as follows. For a black painted cold surface, the total heat flux through the MLI blanket with slots,  $Q_{c,b} = 2.74$  W, the total heat flux through a blanket without slots,  $Q_{o,b} = 1.40$  W, the increment of heat flux due to all slots,  $Q_{s,m}(b) = Q_{c,b} - Q_{o,b} = 1.34$  W. and the increment of heat flux due to unit slot area  $Q_{s,m}(b)/\Delta A = 117.5$  W m².

The ratio of the heat increment due to unit slot area to the heat flux per unit area of black painted surface without MLI  $(Q_b/A = 27 \text{ Wm}^{-2})$  is  $(Q_{s,m}(b)/\Delta A)/(Q_b/A) = 4.3$ 

For an aluminium taped cold surface, the total heat flux through a MLI blanket with slots,  $Q_{c,a} = 2.8$  W, the increment of heat flux due to total slots,  $Q_{s,m}(a) = 1.4$  W, and the increment of heat flux due to a unit slot area,  $Q_{s,m}(a)/\Delta A = 122$  W m<sup>-2</sup>. The ratio of the heat increment due to a unit slot area to the heat flux per unit area of aluminium taped surface without MLI  $(Q_a/A = 4.8 \text{ W m}^{-2})$  is

$$(Q_{s,m}(a)/\triangle A)/(Q_a/A) = 25.4$$

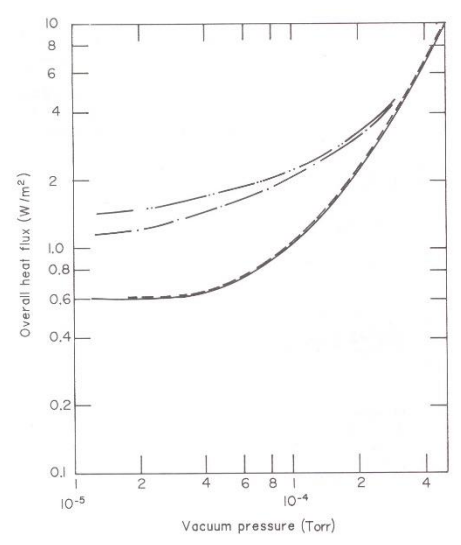
These results agree with the prediction of the enhanced black cavity model: the increments of heat flux due to the slots were almost the same which shows that it is not a function of the cold surface emissivity.

#### Effect of slot width on heat flux

The heat load to a black painted cold surface through a 30 layer MLI blanket with slots was measured with the slot width as a parameter. The widths were varied from zero, a one-dimensional slit, to 30 mm.

*One-dimensional slit*. Fourteen one-dimensional slits were cut to the geometry shown in Figure 1. The heat flux versus vacuum pressure is plotted in Figure 4, along with earlier data without slits. It is clear that one-dimensional slits do not increase the heat flux through a MLI blanket but make evacuating easy.

*Two-dimensional slots.* The measured heat load through a MLI blanket with 2, 4, 6, 9, 15 and 30 mm slots is plotted as a function of slot width in Figure 5. The slope of the curve up to a slot width of ≈ 2 mm was 33.5 W m<sup>-3</sup>; for widths between 2 and ≈ 9 mm the slope was 243 W m<sup>-3</sup>; above 9 mm it was 179 W m<sup>-3</sup>. Figure 6 shows the increment of heat flux per unit slot area as a function of the slot width. The increment of heat flux per unit slot area increases rapidly with width to a broad maximum of ≈ 135 W m<sup>-2</sup> at 9 mm and then decreases gradually.



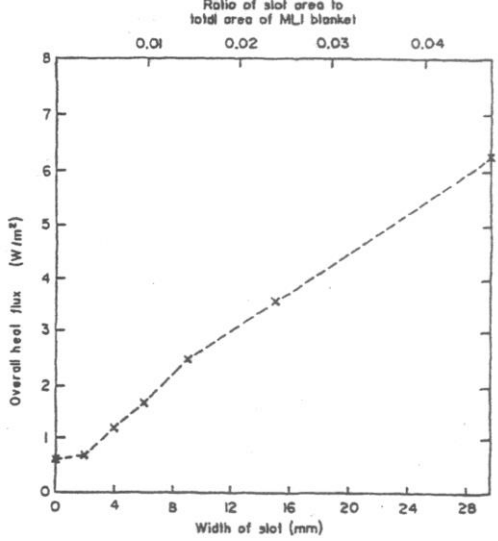
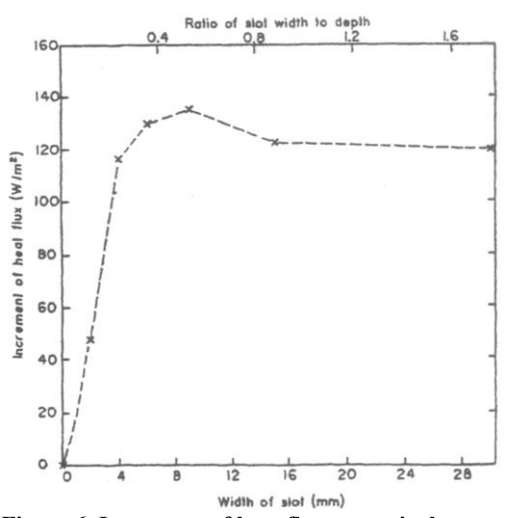


Figure 4 Heat flux as a function of overall vacuum level.
----, Results without cracks;—, Vesults for one – dimeusion al slots;—, 4mm slots;—, square holes

Figure 5 Heat load as a function of slot width for exposed slots

# Effect of crack geometry on heat flux

The square holes cut in the MLI blanket had the same geometric distribution and the same area as the 4 mm slots (see Figure 2). The experimental data for the square holes shows that the overall heat flux at  $2 \times 10^{-5}$  Torr is 1.57 W, and the increment of heat flux per unit crack area is 149 W m<sup>-2</sup>, which is a little larger than that caused by 4 mm slots. Figure 4 shows that at low vacuum pressure the square hole is associated with a greater heat flux than is an equal-area slot, but that the difference decreases with vacuum pressure. For convenience of reference, Table 1 lists all of the beat transfer parameters discussed above.



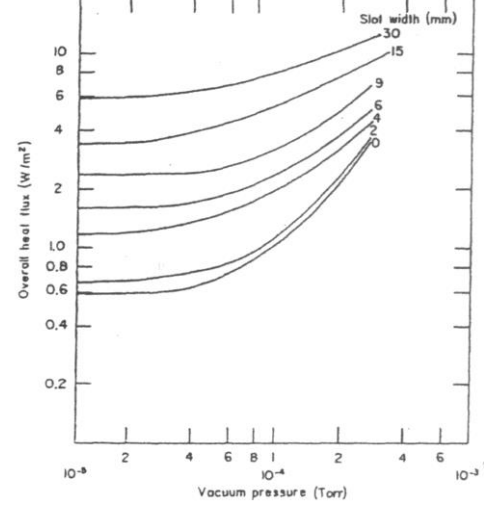


Figure 6 Increment of heat flux per unit slot area as a function of slot width for exposed slots

Figure 7 Heat flux as a function of overall vacuum level for exposed slots of various widths

	Table 1 Thermal transfer parameters for MLI blankets with different crack geometries								
layo	ack geometry in 30 er MLI blanket, d surface tracteristics	Heat load, Q(W)	Overall heat flux (W m <sup>-2</sup> )	Change in overall heat load due to cracks, Q <sub>s.m</sub> (W)	Measured area of crack (m <sup>2</sup> )	Crack area Total area	Change in leat load per unit crack area, Qs.m/△A	$\frac{Q_{s,m}/\Delta A}{Q_{s,m}/A}$	
1	No cracks	$1.40(Q_0)$	0.62	-	-	-	-	-	
2	Slit,painted	1.39	0.62	pprox 0	-	-	-	-	

3	2 mm slot,	1.58	0.69	0.18	0.0038	$1.7 \times 10^{-3}$	47	1.7
4	4 mm slot,painted	2.74	1.2	1.34	0.0114	$5.0 \times 10^{-3}$	117.5	4.3
5	4 mm aluminium taped	2.8	1.23	1.4	0.0114	$5.0 \times 10^{-3}$	122	25.4
6	Square hole, painted	3.58	1.57	$2.08^{b}$	0.014	$6.2 \times 10^{-3}$	149	5.5
7	6 mm slot, painted	3.75	1.65	2.35	0.0181	$8.0 \times 10^{-3}$	129.8	4.8
8	9 mm slot, painted	5.59	2.46	4.19	0.031	$1.4 \times 10^{-3}$	135.2	5.0
9	15 mm slot,	8.02	3.53	6.62	0.054	$2.4 \times 10^{-3}$	122.6	4.5
10	30 mm slot, painted	14.3	6.30	12.9	0.1061	$4.7 \times 10^{-3}$	120.1	4.3

<sup>\*</sup>Oa used here instead of Ob

## Effect of vacuum pressure on overall heat flux for different slot widths

The overall heat flux through MLI blankets with various widths is plotted as a function of vacuum pressure in Figure 7.

#### EXPERIMENTAL RESULTS: (2) REDUCING THE EFFECTS OF CRACKS

Alongside the study into the effects of cracks on the thermal performance of a typical MLI system as background, the use of aluminized Mylar patches to reduce the effect was investigated. A slot width of 4 mm was chosen for this investigation.

#### **OPTIMUM PATCH DISTRIBUTION - FLAT DAM PATCHES**

Four runs were made using DAM patches distributed through the MLI blanket. The distribution and relative results are given in Table 2. It can be seen that, in general, DAM patches can be very effective in reducing the effect of cracks. A few patches in the outer (warm) half of the blanket are as effective as a uniform distribution of patches and better than patches in the inner (cold) half. Figure 8 shows the heat flux as a function of vacuum pressure for different patch arrangements. The dependence of heat flux on vacuum pressure resembles that in a blanket without slots. As shown in Figure 9 the heat flux drops sharply for the first few patches and then approaches the no-slot value.

Table 2 DAM patch distribution and results

Run		Number of patches	Location of patches	Normalized Heat flux <sup>a</sup>
1	No slots	-	-	1.0
2	4 mm slot	0	-	1.9
3		1	After layer 30	1.4
4		4	After layers 15,20,25,30	1.0
5		4	Aftre layers 5,10,15,30	1.3
6		6	Aftre layers 5,10,15,20,25,30	1.0

<sup>&</sup>lt;sup>a</sup> The flux from different patch arrangements divided by the flux with neithar slots nor patches

<sup>&</sup>lt;sup>b</sup>For this run  $Q_0 = 1.5 \text{ W}$ 

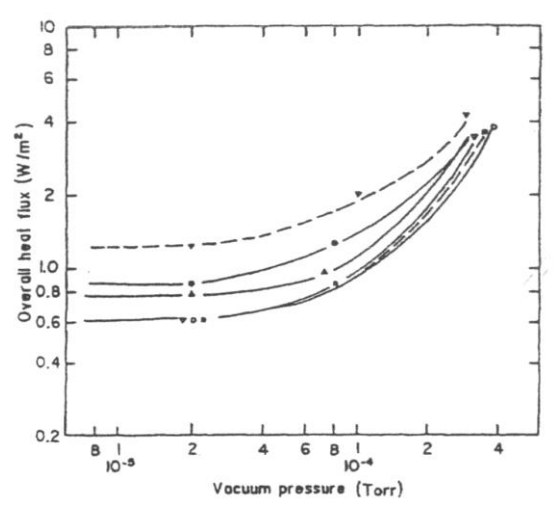


Figure 8 Heat flux as a function of overall vacuum level for slots with DAM patches.  $\bigcirc$ , No slots;  $\blacktriangledown$ , slots without patches;  $\bullet$ , single patches after layer 30;  $\triangledown$ , patches after layers 15, 20, 25, 30;  $\triangle$ , patches after layers 5, 10, 15, 30;  $\square$ , patches after layers 5, 10, 15, 20, 25, 30

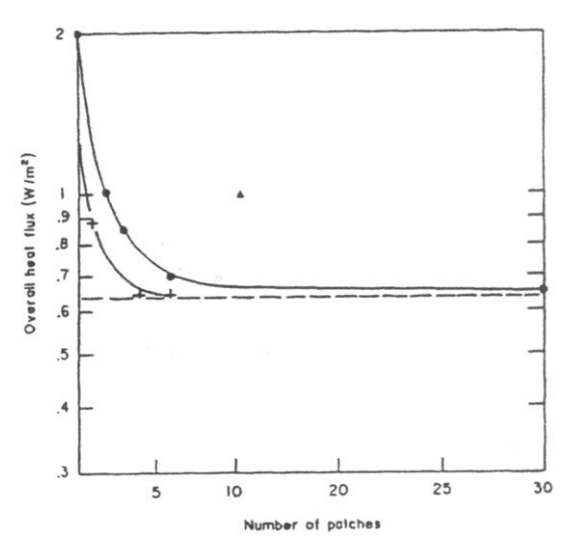


Figure 9 Heat flux as a function of number of patches. +, DAM; ●, SAMC; ▲, 10 patches after layer 30, - - -, Results without cracks

## Optimum number of patches- SAMC patches

Since it was obvious that placing patches in the warmer part of the MLI blanket was more effective in reducing the effect of cracks, a series of runs were made to determine the best number of patches to use. The distribution of the patches and relative results are given in Table 3. It appears that between four and six patches is the minimum necessary to achieve a significant reduction in the heat flux and that the effect becomes marginal above six. The optimum, for this geometry at least, is six patches. This is shown in Figure 9. The overall heat flux as a function of vacuum pressure is given in Figure 10.

Table 3 SAMC patch distribution and results

Run		Number of patches	Location of patches	Normalized Heat flux <sup>a</sup>
1	No slots	-	-	1.0
2	4 mm slot	0	-	1.9
7		30	After layer	1.06
8		6	After layers 5,10,15,20,25,30	1.08
9		3	Aftre layers 20,25,30	1.4
10		2	Aftre layers 25,30	1.6
11		10	Aftre layers 30	1.6

### Patch material

The heat fluxes measured in runs 4 and 9 suggest that  $2 \times 500$  Å DAM might be more effective than 300 Å SAMC. The data from runs 6 and 8, for an identical, uniform distribution of patches, shows quite clearly that  $2 \times 500$  Å DAM is preferable.

#### Patches on square hole

Four DAM patches were used to cover the square holes, after the fifteenth, twentieth, twenty-fifth and thirtieth layers. This reduced the overall heat flux from 1.57 to 0.83 W m<sup>-2</sup>, and the normalized heat flux to 1.0, which is the same as that for four DAM patches on slots of the same area. The overall heat flux as a function of vacuum pressure is shown in Figure 11.

#### Summary of results

All the heat flux data from the study of patches on slots are given in Figure 12 in such a way that the conclusions are self-evident.

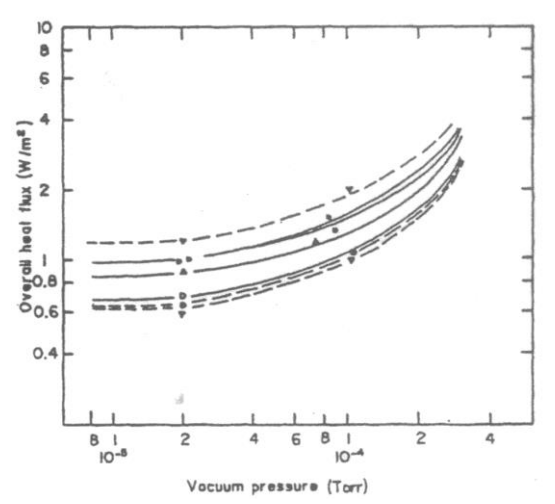


Figure 10 Heat flux as a function of overall vacuum vacuum pressure for slots with SAMC patches.  $\nabla$ ,No slots; DAM

 $\nabla$ , slots without patches;  $\bullet$ , patches after every layer;  $\bigcirc$ , patches after layers 5,10,15,20,25,30;  $\triangle$ , patches after layers 20,25,30;  $\square$ , patches after layers 25 and 30;

■,10 patches after layer 30

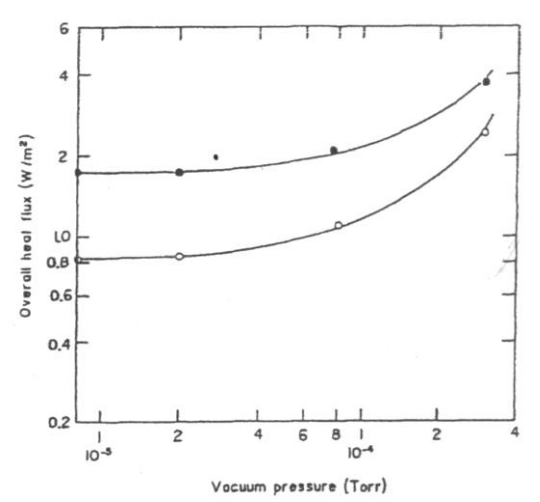


Figure 11 Heat flux as a function of overall pressure for square holes. •, No patches; O, patches after layers 15,20,25,30

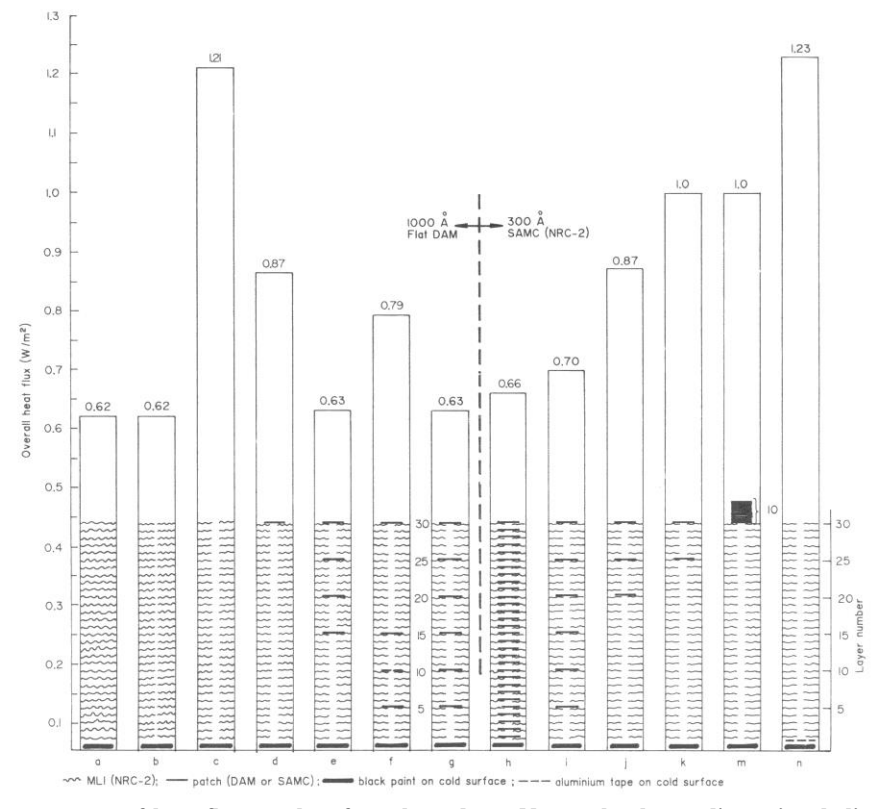


Figure 12 Graphic summary of heat flux results of patch study. a, No cracks; b,one-dimensional slits;c-m,runs 2 to 11; n,0.09mm aluminium tape on cold surface, no patches

#### THERMAL CONDUCTIVITY

The temperature distribution in the MLI blanket was measured for each experimental arrangement as a function of vacuum pressure. As stated before, there are two sides to our MLI blanket: a front side with slots; and a back side without slots. The temperatures in the back-side blanket, shown in Figure 13. are seen to be independent of the slot width. The following discussion concerns only the temperature distributions in the side with slots or square holes since the distribution associated with slits is almost the same as with no cracks.

### Effect of slot width

Table 4 shows the temperature in layers 5 and 15 of a 30 layer MLI blanket with slot widths of 0, 2, 4,6, 9, 15 and 30 mm. The temperature of layers close to the cold plate, the fifth layer for example, initially decreased and then increased as the slot width increased. The temperature of the fifteenth layer always decreased with increasing slot width. The temperatures of the fifth and fifteenth layers in a blanket with slots are compared to those without slots in Figure 14.

In the case of a blanket with slots, the overall heat transfer will change with the size of slots. One can not use

$$K_{ij} = (Q/AD(i,j)) \times [\triangle N/\triangle T]$$
 (1)

directly but one can find the relative change of the equivalent thermal conductivity for different parts of the blanket. Figure 15 is an idealized and parameterized temperature distribution from cold plate through the fifteenth layer.

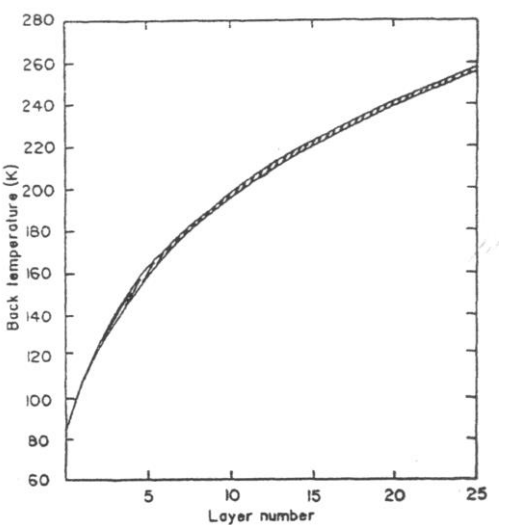
$$\frac{K_{5,15}(9)}{K_{0,5}(9)} = \frac{2\Delta T_{0,5}(9)}{\Delta T_{5,15}(9)} = \frac{2AC}{CD}$$
 (2)

$$\frac{K_{5,15}(0)}{K_{0,5}(0)} = \frac{2\Delta T_{0,5}(0)}{\Delta T_{5,15}(0)} = \frac{2AB}{BE}$$
 (3)

$$\frac{K_{5,15}(9)}{K_{0.5}(9)} \frac{K_{5,15}(0)}{K_{0.15}(0)} > 1$$
 (4)

where:

 $K_{0,5}(9)$  = equivalent thermal conductivity between layer 0 and layer 5 in blanket with 9 mm slots;  $K_{5,15}(9)$  = equivalent thermal conductivity between layer 5 and layer 15;



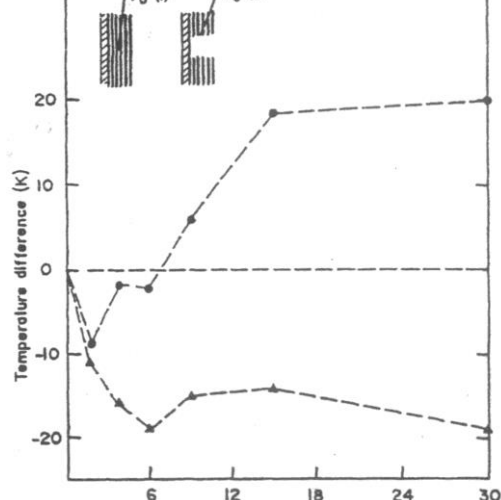


Figure 13 Temperature distribution in back-side blanket. The variations of the back temperatures as a function of slot width fall within the cross-hatched area

Figure 14 Temperature difference  $[T_s(i)-T_o(i)]$  as a function of exposed slot width.  $\bullet$ , Fifth layer;  $\blacktriangle$ , fifteenth layer

 $K_{0,5}(0)$  = equivalent thermal conductivity bewteen layer 0 and layer 5 in blanket without slots; and  $K_{5,15}(0)$  = equivalent thermal conductivity between layer 5 and layer 15 in blanket without slots. Equation (4) shows the relative ratio of the equivalent thermal conductivity in a MLI blanket with slots to that in a blanket without slots. Figure 16 shows that the equivalent thermal conductivity of the blanket near the slots

as a function of slot width varies from  $\approx 30$  to 80 mW cm<sup>-1</sup> K<sup>-1</sup>.

Table 4	<b>Temperatures</b>	in lavers	5 and 15 at	different width of slots
---------	---------------------	-----------	-------------	--------------------------

Width of slot	Temper	Temperature in layer 5 (K)		rature in layer 15 (K)
(mm)	With slot	Without slot	With slot	Without slot
0	183	183	233	233
2	174		222	
4	182		218	
6	181		216	
9	189		218	
15	199		215	
3.0	202		214	
Squarea	178		223	

<sup>&</sup>lt;sup>a</sup> square hole whose area is equal to the are will 4mm slot

## Slots with flat DAM patches

Figure 17 is the temperature distribution in a MLI blanket with flat patches in different locations covering the 4 mm slots, showing that the temperature distribution is a sensitive function of the location of the patches. Several experimental phenomena can be seen. The temperatures,  $T_p$ , of the first 22 layers in a slotted blanket with patches were always lower than the temperatures,  $T_s$ , in a blanket with exposed slots. However, the temperature of the last layer of a blanket with patches,  $T_p(30)$ , was always higher than  $T_s(30)$ . These temperature differences are given in Table 5 and plotted in Figure 18.

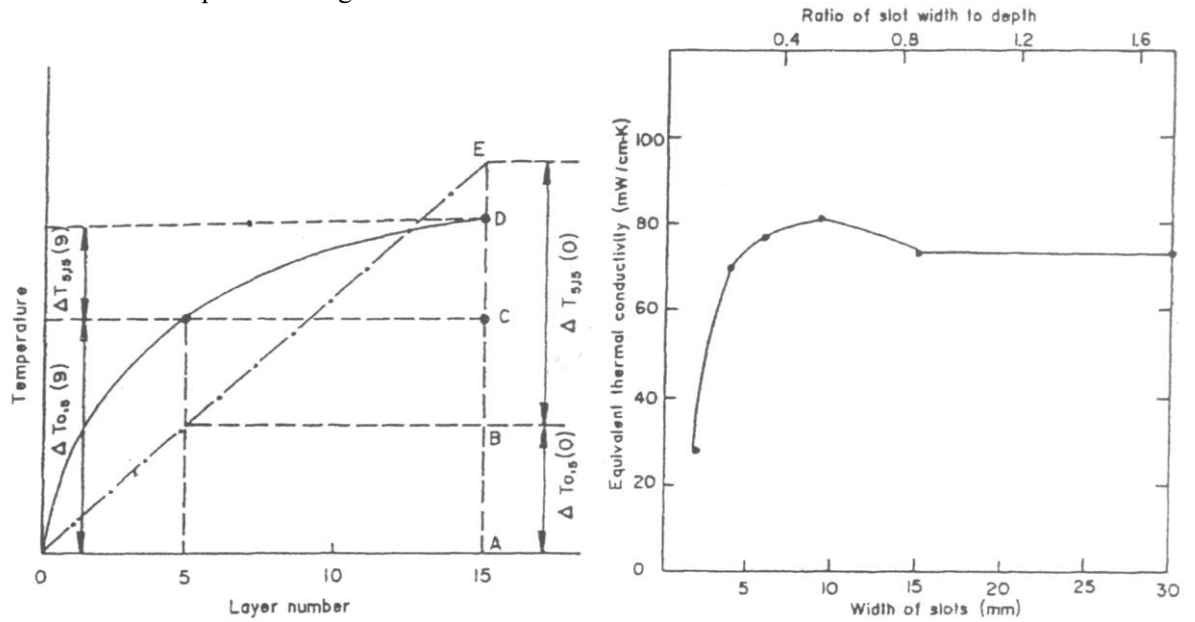


Figure 15 Idealized temperature distribution through layer 15 Figure 16 Equivalent thermal conductivity as a function of slot width. ●, Measured points

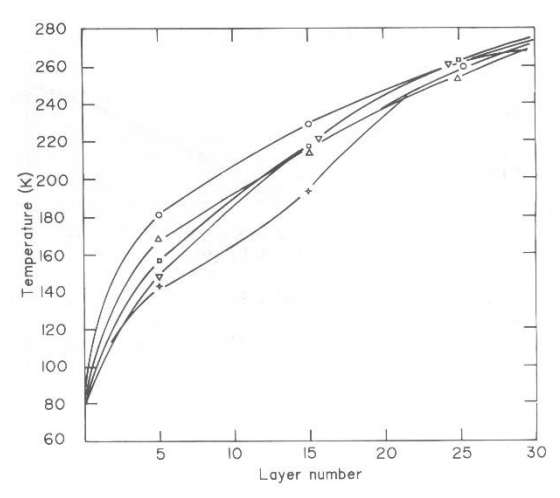


Figure 17 Temperature distributions for slots with for DAM patches.  $\bigcirc$ , Slots without patches;  $\triangle$ , single  $\bullet$ , patches on layer 30;  $\Leftrightarrow$ , patches on layers 15, 20, 25, 15, 20, 30;  $\square$ , patches on layers 5, 10, 15,30;  $\nabla$ , patches on patches layers 5, 10, 15, 20, 25, 30

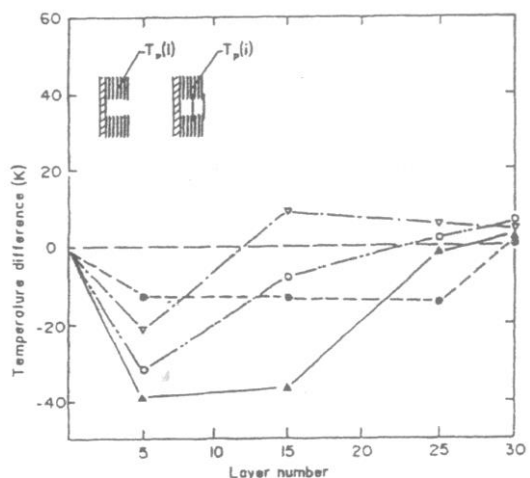


Figure 18 Temperature difference [T<sub>p</sub>(i) - T<sub>s</sub>(i)]

DAM patches as a function of depth in blanket.

Single patches on layer 30; ▲, patches on layers

25, 30; ▽, patches on layers 5, 10, 15, 30; ○,

on layers 5, 10, 15, 20, 25, 30

The local equivalent thermal conductivity, K'(N), for different experimental arrangements was calculated from Figure 17 using

$$K'(N) = \Delta Q / A \times 1 / \Delta T$$

$$K'(N) = K(N) \times D(N)$$
(5)

where K(N) is the thermal conductivity between layer N and N + 1. K'(N) is plotted in Figure 19 as a function of depth in the blanket. Another interesting feature is that when patches are located in the warm half of the blanket, the local equivalent conductivity exhibits a maximum value around the twelfth layer (before first patch from cold plate) and a minimum around the sixteenth layer (after the first patch from cold plate).

Table 5 Temperature differences in layer 30

Type of crack	Patch material	Number of patches	Location of patches (layer number)	$\triangle T(K)$	T <sub>P</sub> (30) (K)
4 mm slot	1000 Å,DAM	1	30	2.7	271.8
4 mm slot	1000 Å,DAM	4	30,25,20,15	4.5	273.7
4 mm slot	1000 Å,DAM	4	30,15,10,5	3.9	273
4 mm slot	1000 Å,DAM	6	30,25,20,15,10,5	4.9	274
4 mm slot	300Å,DAM	30	Every layer	4.1	273.2
4 mm slot	300 Å,DAM	6	30,25,20,15,10,5	3.9	273
4 mm slot	300 Å,DAM	3	30,25,20	3.4	272.5
4 mm slot	300 Å,DAM	2	30,25	2.6	271.7
4 mm slot	300 Å,DAM	10	30	-14.1	255
Square hole	-	0	-	-3.3	268.8
Square hole	1000 Å,DAM	4	30,25,20,15	2.9	272
4 mm slot,Aluminium Taped cold fin	-	0		3	272.1

 $T_p(30)$ : temperature of patch on thirtieth layer

 $T_s(30)$ : temperature of exposed thirtieth layer = 269.1 K

 $\triangle T = T_P(30) - T_s(30) = T_p(30) - 269.1 \text{ K}$ 

#### Slots with SAMC patches

Figure 20 shows the temperature distribution in a MLI blanket with SAMC patches covering 4 mm slots for different patch arrangements. The distributions are quite similar to those obtained with flat patches. The

temperature in the last layer of a blanket with crinkled patches is higher than that without patches (see Table 5). The temperature difference between layers with exposed slots and those covered with crinkled patches is plotted in Figure 21, which shows that  $T_p$  is lower than  $T_s$ , except in the region close to the last layer. It should be noted that the temperature of the last layer of a blanket with ten patches placed on the top of the slot is 14 K lower than that without any patches. The local equivalent thermal conductivity for different arrangements of SAMC patches is given in Figure 22. In this case several of the arrangements result in a maximum conductivity around the middle of the blanket.

Square holes with SAMC patches and slots with aluminium taped cold surface. Temperature distributions were also measured for square holes with and without patches and for 4 mm slots in a blanket over a taped cold surface, and are shown in Figure 23. The distribution for the square holes is quite similar to that found for slots of the same area. The corresponding temperature differences are shown in Figures 24 and 25.

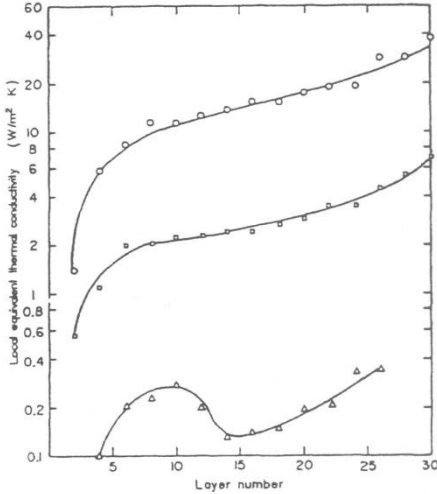


Figure 19 Local equivalent thermal conduc SAMC tivity for slots with DAM patches as a function of depth in blanket. ○, Slots without patches; □, patches after layers 15, 20, 25. 30; △, patches after layers 5, 10, 15, 30

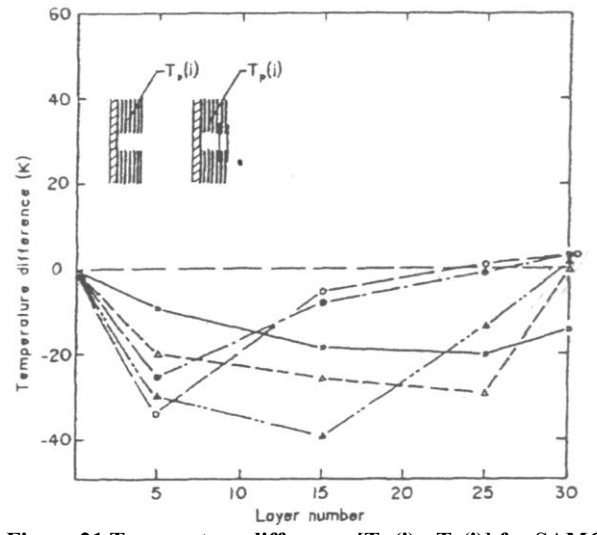
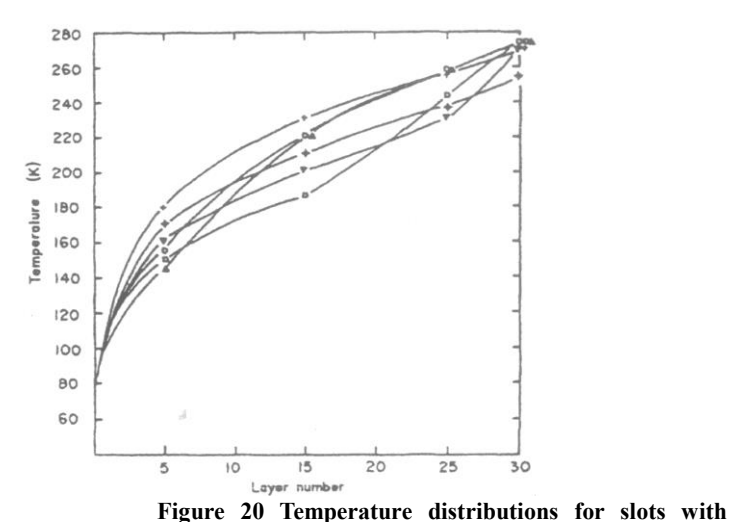


Figure 21 Temperature difference [Tp(i) - Ta(i)] for SAMC conductivity patches as a function of depth in blanket. ●, Patches after blanket. every layer;, ○, patches after layers 5, 10, 15, 20, 25, 30;



rigare 20 remperature distributions for slots with

patches. +, Slots without patches;  $\bigcirc$ , patches after every layer;  $\triangle$ , patches after layers 5, 10, 15, 20, 25, 30;  $\square$ , patches after layers 20, 25, 30;  $\nabla$ , patches after layers 25 and 30;  $\stackrel{\triangleright}{\hookrightarrow}$ , 10 patches after layer 30

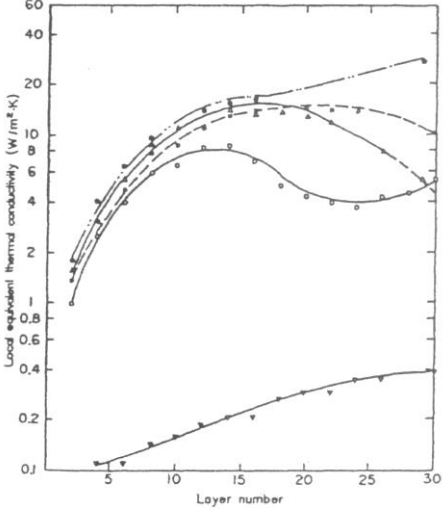


Figure 22 Local ∇equivalent thermal for SAMC patches as a function of depth in 

■, Slots withoul patches; , patches after every

layer;

 $\triangle$ , patches after layers 20, 25, 30; A, patches after layerS 25 and 30;  $\square$ , 10 patches after layer 30 layer 30

O, patches after layers 20, 25, 30;  $\triangle$ , patches after layers 25 and 30;  $\Box$ , 10 patches after

# Effect of vacuum pressure

Figures 26 and 27 give the temperature distribution as a function of vacuum pressure for a MLI blanket with 4 mm slots different flat patch arrangements. It can be seen that the temperature distribution changes more for slots than for patched slots as the vacuum pressure increases. The distributions for slots covered with SAMC patches are given in Figures 28, 29 and 30. Figure 31 gives the distributions for square holes and Figure 32 for 4 mm slots with an aluminium taped cold surface.

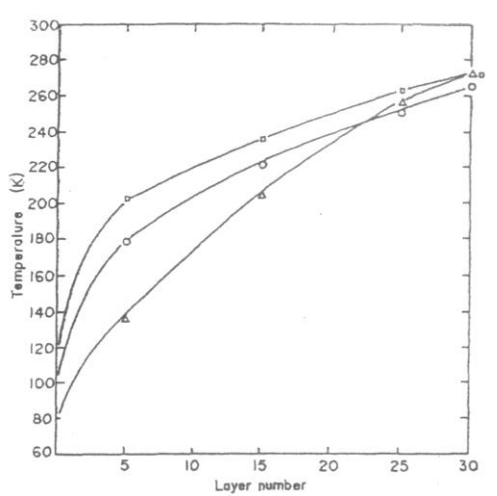


Figure 23 Temperature distributions for square square holes

holes with DAM patches and for slots over taped patches

cold surface.  $\bigcirc$ , Square hole without patches;  $\triangle$ , 30.

square hole with patches after layers 15, 20, 25, 30;  $\Box$ , 4 mm slot with aluminium tape on cold surface, no patches

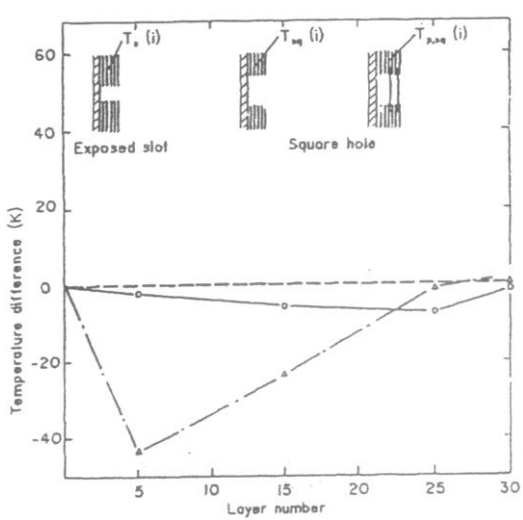
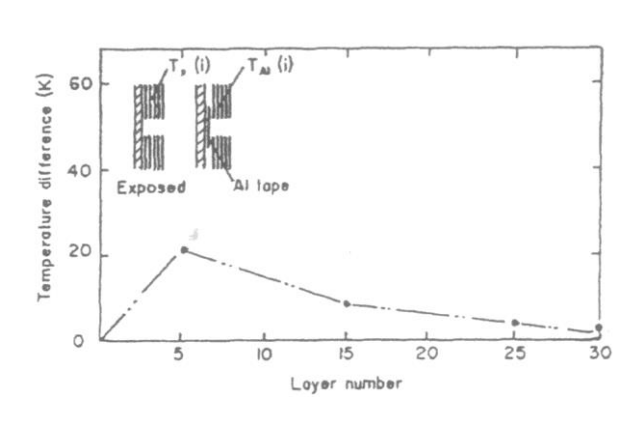


Figure 24 Temperature difference for

as a function of depth in blanket. O, Without

-  $T_{sq}(i)$  -  $T_{s}(i)$ ;  $\triangle$ , patches after layers 15, 20, 25,

 $T_{p,sq}(i) - T_s(i)$ 



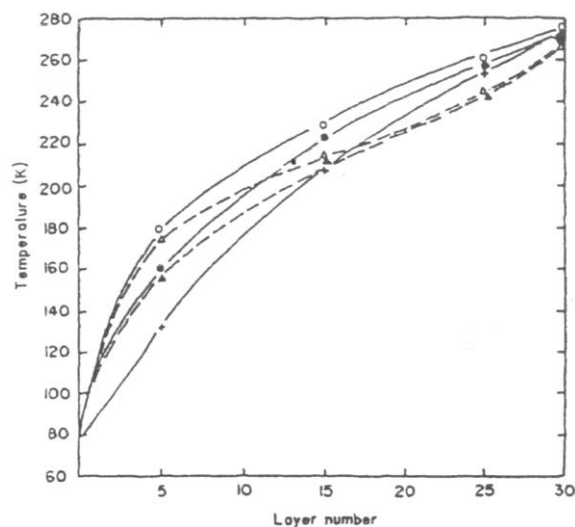
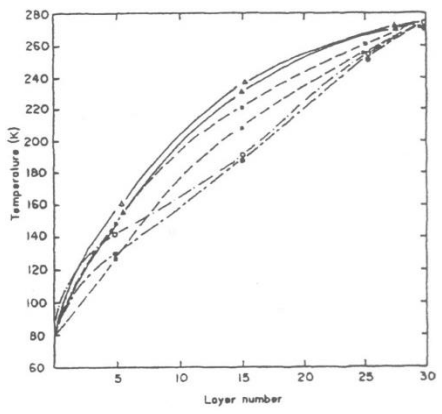


Figure 25 Temperature difference for slots with taped cold Figure 26 Temperature distributions for exposed slots surface as a function of depth in blanket.  $\bullet$ ,  $T_{AI}(i) - T_s(i)$  ( $\circlearrowleft$ ,  $\bullet$ ) and for slots with single patches on layer 30 ( $\bigtriangleup$ ,  $\blacktriangle$ ) as function of vacuum pressure.  $\circlearrowleft$ ,  $\bigtriangleup$ ,  $2 \times 10^{-5}$  Torr;  $\bullet$ ,  $\bigstar$ ,  $8 \times 10^{-5}$  Torr;  $\diamondsuit$ ,  $3 \times 10^{-4}$  Torr



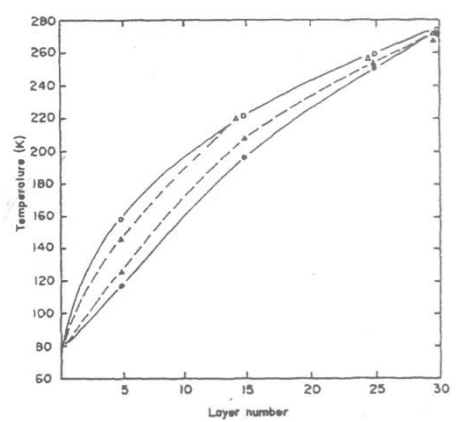
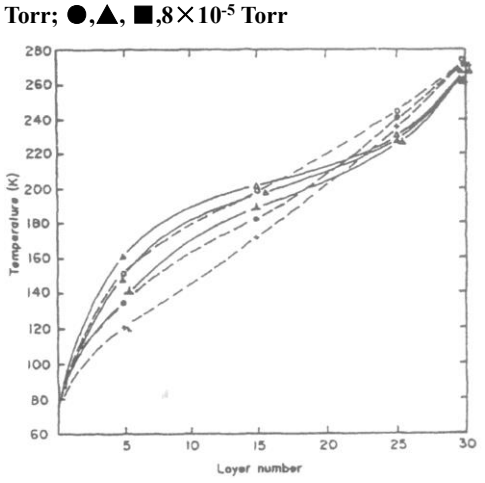


Figure 27 Temperature distributions for slots with DAM

Figure 28 Temperature distributions for slots

patches as a function of vacuum pressure. O, , Patches after layers  $15,20,25,30; \triangle, \blacktriangle$ , patches after layers 5,10,15, 30;  $\square$ , patches after layers 5,10,20,25,30;  $\bigcirc$ ,  $\triangle$ ,  $\square$ ,2×10<sup>-5</sup> 20,25,30;  $\bigcirc$ ,  $\triangle$ , 2×10<sup>-5</sup> Torr;  $\triangle$ , 8×10<sup>-5</sup> Torr;

SAMC patches as a function of vacuum pressure. O, •, Patches after layer;  $\triangle$ ,  $\triangle$ , patches after layers 5,10,15,



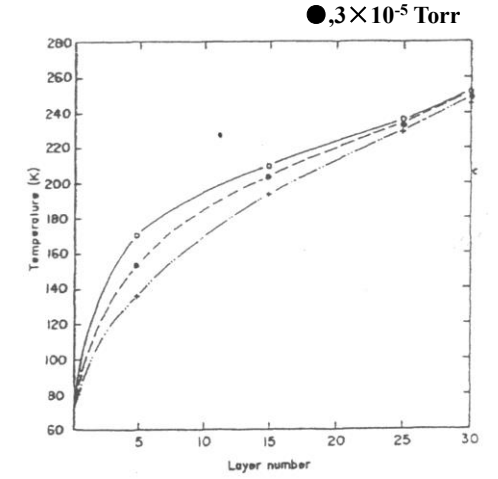
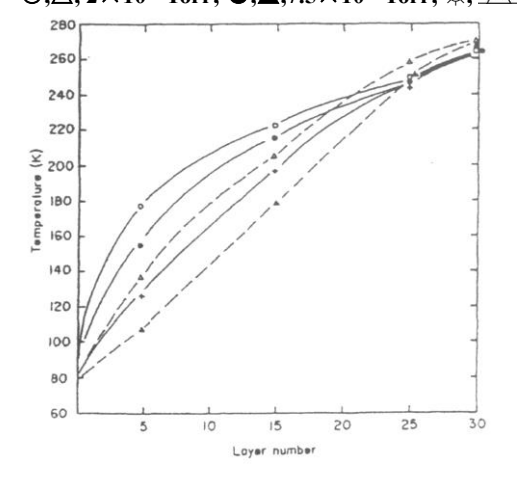


Figure 29 Temperature distributions for slots with SAMC Figure 30 Temperature distributions for slots with patches as a function of vacuum pressure. O, ●, ♥, Patches SAMC patches as a function of vacuum pressure. O, after layer 20,25,30;  $\triangle$ ,  $\triangle$ , patches after layers 25 and 30;  $2 \times 10^{-5}$  Torr;  $\bigcirc$ ,  $8 \times 10^{-5}$  Torr;  $\bigcirc$ ,  $3.2 \times 10^{-4}$  Torr  $\bigcirc, \triangle, 2 \times 10^{-5} \text{ Torr}; \bullet, \blacktriangle, 7.5 \times 10^{-5} \text{ Torr}; \heartsuit, \triangle, 3 \times 10^{-4} \text{ Torr}$ 



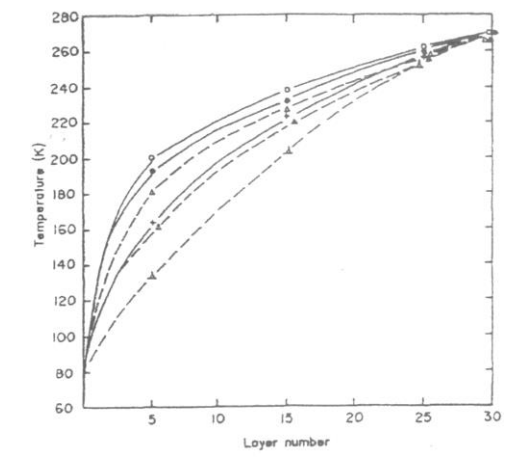


Figure 31 Temperature distributions for square holes with DAM patches as a function of vacuum pressure;  $\bigcirc$ ,  $\bigcirc$ ,  $\rightleftharpoons$ , Exposed holes;  $\triangle$ ,  $\triangle$ , patches on layers 15,20,25,30.  $\bigcirc$ ,  $\triangle$ ,2×10<sup>-5</sup> Torr;  $\bigcirc$ , Torr

Figure 32 Temperature distributions for exposed slots over aluminium taped( $\bigcirc$ ,  $\bigcirc$ ,  $\Rightarrow$ ) and black painted ( $\triangle$ ,  $\triangle$ ,  $\triangle$ ) cold surfaces as a function of vacuum pressure;  $\bigcirc$ ,  $\triangle$ ,  $2 \times 10^{-5}$  Torr;  $\bigcirc$ ,  $\triangle$ ,  $8 \times 10^{-5}$  Torr;  $\Leftrightarrow$ ,  $3 \times 10^{-4}$ 

7.6×10<sup>-5</sup> Torr; ▲ 3×10<sup>-4</sup> Torr

#### DISCUSSION

When installing a MLI blanket on a cryogenic device patches should be used to cover the crack in each layer if possible. However, if a crack exists in an already installed blanket the retrofitting of patches will depend on how easily patches may be installed without damaging or disturbing the structure of the original blanket, it is widely known that there is an optimum distribution for radiation shields in an insulation vacuum space of a cryogenic device. The optimum patch distribution which we observed showed that there are similarities and differences between patches and shields. The enhanced blank cavity model suggests that a uniform distribution of patches is preferable and also that patches distributed in the outer half of a blanket would be much better than the inner half because the former interrupts the radiation flux at a warmer temperature. It is also probably easier to retrofit patches into the outer half.

The experimental results from crinkled Mylar (Figure 9) showed that the overall heat flux decreased rapidly as the number of patches was increased and rather quickly approached the value in a system without cracks. The slope of Figure 9 is greater than that observed by increasing the number of layers in a system free of cracks<sup>4</sup>. Between six and 10 patches the overall heat flux is almost equal to that for a patch after each layer. This is the reason that we recommended using a few patches instead of one for each layer especially where it is difficult to install patches into the inner section of the MLI blanket.

The increment of heat flux versus the width of the slots, shown in Figure 6, demonstrated experimentally the effect of a cavity degrading the effectiveness of a black cavity. Since the effectiveness of a black cavity decreased with increasing slot width, the increment of heat flux due to unit slot area decreased gradually with increasing the width of slot after a certain value. It can also be seen from Figure 6 and Table 1 that the effect of the black cavity will disappear as the slot width approaches zero.

Our experiments showed that the temperature distribution in MLI near cracks is a sensitive function both of the dimension of the crack and of the location and number of patches. These results indicated that the existence of a crack changes the entire temperature field of the MLI blanket which increases the heat flux. Based on the experimental data several additional remarks on the temperature distribution can be made. It can be seen from Table 4 that the temperature in the colder section decreases slightly for slot widths  $\approx 2$  mm and then increases gradually with increasing slot width. However, the temperature in the middle part (around layer 15) will decrease with increasing slot width. One observes from Figures 17 and 20, that the temperature near a slot with a patch is lower than near a slot without a patch in most of the MLI blanket, From Table 5 we note that the temperature in the last patch (on the warmest layer) is an indication of the improvement in the thermal performance resulting from patches. Basically, the higher the temperature of the last patch, the less the heat flux going through the crack. Figures 19 and 22 show that the local equivalent thermal conductivity of a crack changes with the depth in the MLI blanket and that the overall equivalent thermal conductivity decreases as the number of patches is increased. If the number of patches used in a crack is the same, the equivalent thermal conductivity with the patches in the outer half of the blanket is less by about an order of magnitude than that observed with the patches in the inner half.

#### **CONCLUSIONS**

The thermal performance of a MLI blanket is widely known to be a sensitive function of the material, the geometry of the device and craftsmanship<sup>13-17</sup>. The quantitative effects of cracks is likewise dependent on these same factors. Nevertheless, the experimental results presented here lead to conclusions which should be of general interest. These conclusions can be summarized as follows:

1 a crack in a MLI blanket will cause a significant increase in the heat flux. The mean equivalent thermal

conductivity of a narrow crack is  $3-8 \text{ W m}^{-1} \text{ K}^{-1}$ . The increase in heat flux due to unit crack area is a function of the aspect ratio of the crack with a maximum of  $149 \text{ W m}^{-2}$ ;

- 2 the use of aluminized Mylar patches to cover the crack at each layer is good but may not be easy to install. However, the use of flat, DAM, 1000Å patches on a few layers will give almost the same improvement as patches between each layer. Placing the patches in the outer (warmer) half of the blanket is much better than in the inner (colder) half. Putting patches on the outside of the crack is not very effective;
- 3 Mylar with more aluminizing (1000 Å) is better as a patch material. Crinkled Mylar with 300-500 Å single aluminizing is easier to install since spacers are not required;
- 4 reducing the emissivity of the cold surface under a narrow crack does not significantly effect the heat flux;
- 5 the presence of cracks and patches changes the temperature distribution in the MLI blanket near the cracks. The temperature of the layer closest to the cold surface increased and that of the layer closest to the warm surfaces decreased as the width of the slots increased. Patches make the temperature of the MLI blanket near a crack lower than that for an exposed slot. The higher temperature of the last (warmest) patch indicates the ability of a patch system to protect the cold surface against incoming radiation;
- 6 the local equivalent thermal conductivity of a crack is a sensitive function of the distribution and number of patches along the crack. It is a minimum around the first patch from the cold surface and a maximum a few layers after the first patch, while installing patches on the warm half of the MLI blanket; and
- 7 the experimental results are generally in agreement with the enhanced black, cavity model.

#### REFERENCES

- [1] Shu, Q.S. Systematic study to reduce the effects of cracks in multilayer insulation. Part 1: theoretical model Cryogenics (1987) 27 249-256
- [2] Jackson, J.D. SSS conceptual design. SSC-SR-2020. SSC Central Design Group, Berkeley, California, USA (March 1986)
- [3] Preliminary report on the design of the Superconducting Super Collider, prepared by SSC Central Design Group, Universities Research Association, Berkeley, California, USA (January 1986)
- [4] Report on the design of the Fermi National Accelerator Laboratory superconducting accelerator, Fermilab, Batavia, Illinois, USA (May 1979)
- [5] Desportes, H. Superconducting magnets for large accelerators Cryogenics (1985) 25 613-618
- [6] Komarek, P. Superconducting magnets in fusion research Cryogenics (1985) 25 604-612
- [7] Shu, Q.S., Fast, R.W. and Hart, H.L. An experimental study of heat transfer in multilayer insulation system from room temperature to 77 K Adv Cryog Eng Plenum Press, New York, USA (1986) 31 455-463
- [8] Shu Q.S., Fast, R.W. and Hart, H.L. Heat flux from 277 to 77 K through a few layers of multilayer insulation Cryogenics (1986) 26 671-677
- [9] Ecke R.E., Shu, Q.S., Sullivan, T.S. and Vilches, O.E. Phase boundaries and critical and tricritical properties of monolayers<sup>4</sup> He adsorbed on graphite phys Rev B (1985) 31 448-455
- [10] Kropschot,R.H., Schrudt, J.E., Fulk, M.M. and Hunter, B.I. Multiple layer insulation Adv Cryog Eng Plenum Press, New York, USA (1960) 5 189-198
- [11] Mikhalchenko, R.S., Getnanets, V.F., Peshin, N.P. and Batozskii, Yu,V. Study of heat transfer in multilayer insulation based on composite spacer materials Cryogenics (1983) 23 309-311
- [12] Matsuda, A. and Yoshikyo, H. Simple structure insulation material properties for multilayer insulation Cryogenics (1980)20 135-138
- [13] Siegel, R.Thermal radiation heat transfer, NASA SP-164, US Government Printing Office, Washington, DC, USA (1971)
- [14] Balcerek, K. and Rafadowcz, J. The residual gas pressure distribution between layers of superinsulation ICEC 6 IPC Science and Technology Press, Guildford, UK (1976) 255-257
- [15] Chaussy, J., Gianese, P. and Peyrand, J. Reduction of evaporation rate by use of metallic adhesive tape Cryogenics (1976) 16 10-11
- [16] Eyssa, Y.M. and O. Okasha Thermodynamic optimization of thermal shields for a cryogenic apparatus Cryogenics (1978) 18 305-307
- [17] Leung, E.M.W., Fast, R.W. and Hart, H.L. Techniques for reducing radiation heat transfer between 77 and 4.2 K Adv Cryog Eng Plenum Press, New York, USA (1981) 25 489—499